Journal of Naval Architecture and Marine Engineering
June, 2005
http://jname.8m.net

MODELING OF MARINE GAS TURBINE COMBUSTOR UNDER NON-REACTING AND REACTING CONDITIONS

V. Jyothishkumar [1] and V. Ganesan

[1] Ph.D.scholar, Indian Institute of Technology Madras, Chennai-600 036, India, kumar_jyothish@hotmail.com

[2] Professor, Internal Combustion Engine Laboratory, Department of Mechanical Engineering, Indian Institute of Technology Madras, Chennai-600 036, India, vganesan@acer.iitm.ernet.in

Abstract

Present work is concerned with the flow field analysis inside a marine annular gas turbine combustor under non-reacting as well as reacting flow conditions. Three-dimensional gas turbine combustor of 20-degree sector geometry has been created and meshed using the pre-processor GAMBIT. Flow through the combustor has been simulated using FLUENT code by solving the appropriate governing equations viz. Conservation of mass, momentum and energy. The RNG k-ε turbulence model is used for physical modeling. Combustion has been modeled using the Probability Density Function (PDF) approach. Total pressure loss has been studied for the isothermal as well as reacting flow case. For reacting flow overall pressure loss across the combustor has been evaluated.

Keywords: Combustor, Recirculation region, Non-reacting flow.

NOMENCLATURE:

C_p	Specific heat, J/kg-K	X	Longitudinal distance, m
E	Energy, J	δ	Kronecker-delta function
F	External body force, N	μ	Molecular viscosity, kg/m-s
H	Sensible enthalpy, J/kg	μ_t	Turbulent viscosity, kg/m-s
J	Diffusion flux, kg/m^2-s	ρ	Mean density, kg/m^3
k_{eff}	Effective thermal conductivity,	τ	Shear stress, N/m^2
m_i,	Mass fraction of the species	*eff*	Effective value (laminar +
P	Static pressure, Pa	*i, j, k*	Tensorial notation
T	Temperature, K	X	Longitudinal distance, m
u_i	Mean velocity in j-th direction,		

1. Introduction:

During the last decade, numerical prediction methods have become popular with the availability of fast digital computers and information processing capabilities. Combustor designs are generally guided predominantly by experimental methods and past experiences. However, experimental methods are inherently slow and also very costly especially at engine operating conditions. These drawbacks and the growing need to understand the complex flow field phenomena involved have lead to the development of numerical model for predicting flow in the gas turbine combustors.

A gas turbine combustion chamber must satisfy a wide range of requirements viz., high combustion efficiency, low pressure drop, outlet temperature profile as dictated by the turbine designers, stable combustion over wide range of pressure, velocity and air-fuel ratio and low emissions of pollutants and unburned fuel. Many of the above requirements are conflicting which makes the design of a gas turbine combustor a challenging task. In the past several studies have been made in the area of flow analysis inside a combustion chamber. Ganesan and Spalding (1979) have done numerical modeling of the combustion of fuel sprays in three-dimensional can combustors, Novick et al (1979) performed

the numerical simulation of combustor flow fields with and without reaction. Sampath and Ganesan (1987) analysed the reactive flow field in a combustor, the ability of a finite difference computational procedure to predict the local flow conditions in a three-dimensional gas turbine combustor model. Cameron et al (1989) carried out a detailed characterization of velocity and thermal fields in a model can combustor with wall jet injection. Isaac and Wu (1989) conducted numerical simulation of strongly swirling axisymmetric flow field in sudden expansion geometry. Karki et al (1992) analyzed the dump diffuser by using CFD. Mongia et al (1992) designed combustors using empirical/analytical method. Tolpodi (1995) modeled the two-phase flow in gas turbine combustor and has described the development of a spray combustor model. Sokolov et al (1995) carried out mathematical modeling of annular gas turbine combustor. Alizadeh et al (1996) investigated combustion in gas turbine combustor using CFD. Agarwal et al (1998) carried out an experimental and computational study of the cold flow in the combustor diffuser system of the industrial gas turbine combustors. Maroun et al (2000) carried out a mathematical model capable of describing the evaporation and mixing of a reacting two-phase flow. Han et al (2001) carried out optimum arrangement between a fuel nozzle and a swirler to achieve satisfactory ignition. Balasubramanian and Ganesan (2001) have analysed the gas turbine combustion system using computational procedure. Thus it is seen that there is considerable interest is the design and development of combustion system for gas turbine power plant. The main aim of the present work is to analyse the flow and combustion in a typical marine gas turbine combustor. Marine gas turbine combustors use diesel as fuel. However, in this studies heptane is taken as fuel for combustion since the properties are closer to diesel. It is important to estimate various parameters like velocity, total pressure losses, temperature and species concentration inside the chamber.

2. **Basic Combustor Geometry and its parts**

Basic geometry of combustor with different parts is shown in Fig. 1. Geometry under consideration is shown in Fig. 2. Zoomed view near dome and flare region is shown in Fig. 3. Dome and flare region are shown separately in Fig. 4 and Fig. 6 with zoomed view near the holes in Fig. 5 and Fig. 7. Meshed geometry is also shown in Fig. 8. Zoomed view of meshed geometry is shown in Fig. 9. Total number of tetrahedral cells used for meshing is equal to 2 million.

3. Objective

The objectives of the present work include:

- Modeling the geometry with real holes for dome and flare region, primary and dilution region and in liner region.
- The study of the flow field in the combustor for non-reacting and reacting condition. Estimation of the pressure loss for the combustor geometry under consideration with different inlet velocity.

4. Computational Model and Meshing Complexities

The geometry under consideration is an annular gas turbine combustor. A straight walled pre-diffuser projects into a dump cavity where the flow is divided to pass into the flame tube and the surrounding feed annuli. Fuel is injected into the flame tube by a set of 18 nozzles located at the compressor end of the chamber. The design provides for dividing the air into primary and secondary streams, the former to support combustion in a high temperature turbulent zone and the latter to cool the combustion products so as to bring down the temperature to a value within the operational limits of the turbine. The geometry is as shown in Fig. 1.

Model has been generated using pre-processor GAMBIT. Because of the rotational symmetry, only three-dimensional model of 20-degree sector is considered for modeling. The whole geometry is modeled with thickness of the material wherever necessary and is shown in Fig. 2. The thickness is considered for including the effect of real holes in dome and flare region, primary and dilution zones and in liners. The holes in dome and flare region are about 1mm diameter each. There are about 790 holes in dome region and 678 holes in flare region. There are two primary holes in the outer and inner

annulus. There is only one dilution hole in the outer annulus and two dilution holes in the inner annulus. There are about 200 cooling ring holes in outer and inner annulus. Alternative way of approximating these holes is to provide porous jump boundary conditions in the respective faces where the holes are present. Even though it is difficult to model the real holes, it is to be noted that realistic flow field predictions can be obtained only by modeling holes appropriately.

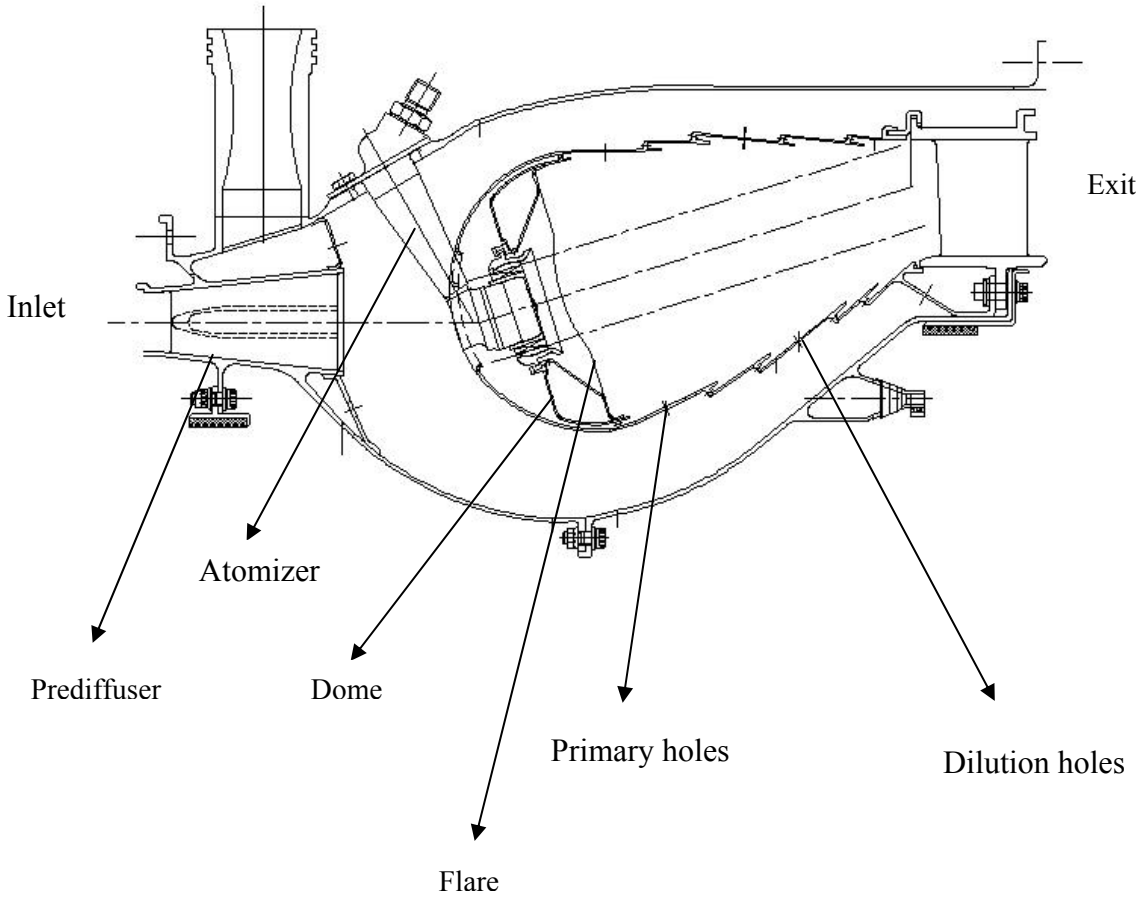

Figure 1: Basic combustor geometry

Meshing the dome and flare holes are very complex. There are six nodes forming a hexagon at each face of the holes covering 85% of the flow area with 36 nodes in each hole with skewness of about 0.6. Unstructured grid of size 2 million tetrahedral cells has been adopted for meshing. Meshed geometry is as shown in Fig. 8.

5. Boundary Conditions

Present computational work involves three types of boundaries. (i) Inlet (ii) Outlet (iii) Wall.

Inlet: Velocity boundary condition is used to define the flow velocity, along with relevant properties of the flow at the flow inlet. Velocity magnitude and direction, the velocity components or the velocity magnitude normal to the boundary specifies inlet velocity boundary conditions.

Wall: In the present case walls are assumed to be adiabatic with no slip condition.

Outlet: Outlet boundary condition is used to model the flow at exit where the details of the flow velocity and pressure are not known prior to solution of the problem. As these variables are not known for the case under study, we have adopted this boundary condition for the combustor exit. When this condition is specified, the code extrapolates the required information from the interior.

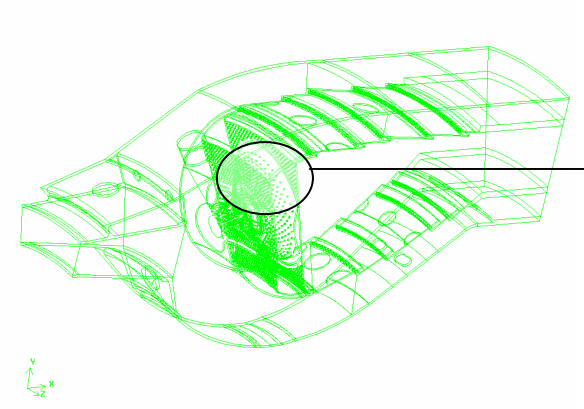

Figure 2: Geometry under consideration

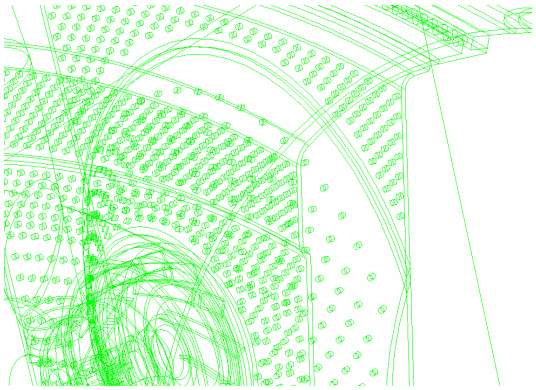

Figure 3: Zoomed view near dome and flare region

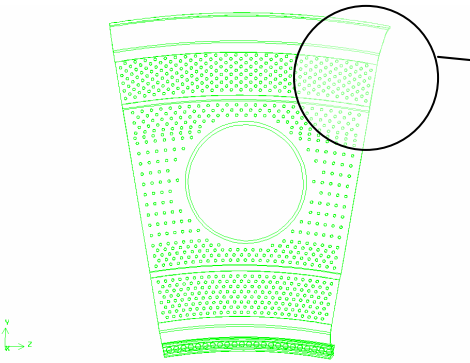

Figure 4: Dome

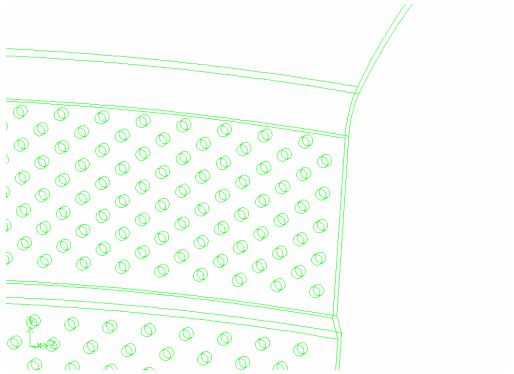

Figure 5: Zoomed view near the dome hole

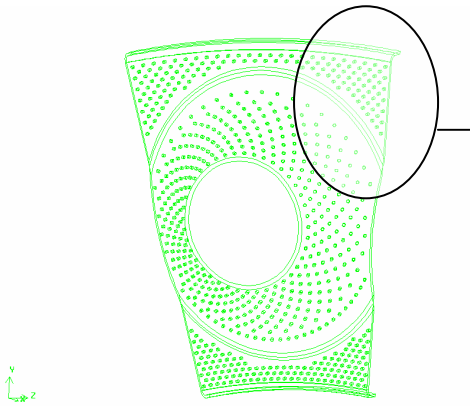

Figure 6: Flare hole

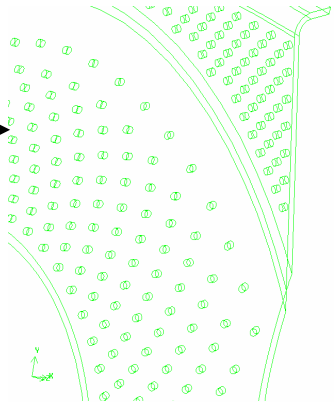

Figure 7: Zoomed view near the flare

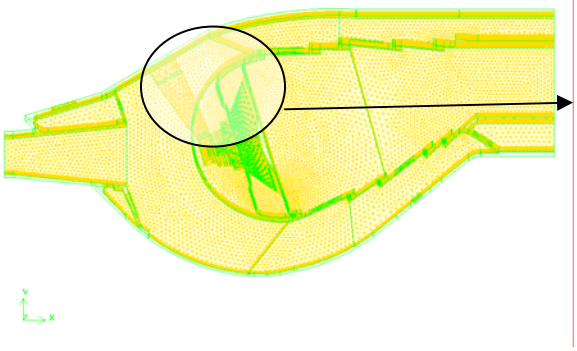

Figure 8: Meshed Geometry tetrahedral cells

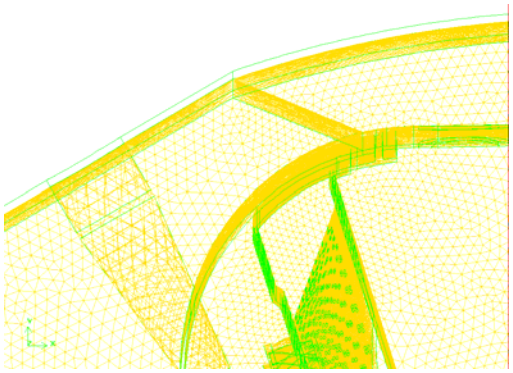

Figure 9: Zoomed view showing

6. Governing Equations

To predict the flow field in a marine gas turbine combustor, the following partial differential equations are to be solved for getting the aerodynamics.

Continuity Equation

$$\frac{\partial}{\partial X_i}(\rho u_i) = S_m \tag{5.1}$$

The source term S_m is the mass added to the continuous phase from the dispersed second phase (due to vaporization of liquid droplets). For the non-reacting flow S_m takes a value of zero.

Momentum Equation

$$\frac{\partial}{\partial X_j}(\rho u_i u_j) = -\frac{\partial p}{\partial X_i} + \frac{\partial}{\partial X_j}\left[\mu\left(\frac{\partial u_i}{\partial X_j} + \frac{\partial u_j}{\partial X_i} - \frac{2}{3}\delta_{ij}\frac{\partial u_i}{\partial X_i}\right)\right] + \frac{\partial}{\partial X_j}(-\rho\overline{u_i' u_j'}) + F_i \tag{5.2}$$

where p is the static pressure, μ the molecular viscosity, δ_{ij} is kronecker-delta function and $\boldsymbol{F_i}$ **is the external body force that arises from interaction with the dispersed phase in the** ***i*** **direction and also include the source term**. The second term in the right hand side represents the stress tensor denoted by τ_{ij}. The third term in the right hand side of the above equation represents Reynolds stresses and these are modelled using Boussinessq hypothesis. According to this hypothesis the Reynolds stresses are related to the mean velocity gradients by

$$-\rho\overline{u_i' u_j'} = \mu_t\left(\frac{\partial u_i}{\partial X_j} + \frac{\partial u_j}{\partial X_i}\right) - \frac{2}{3}\left(\rho k + \mu_t\frac{\partial u_i}{\partial X_i}\right)\delta_{ij}$$

where k is the turbulent kinetic energy and μ_t is turbulent viscosity whose computational method depends on the type of turbulence model used.

Energy Equation

$$\frac{\partial}{\partial X_i}(u_i(\rho E + p)) = \frac{\partial}{\partial X_i}\left(k_{eff}\frac{\partial T}{\partial X_i} - \sum_j h_j J_j + u_j(\tau_{ij})_{eff}\right) + S_h \tag{5.4}$$

where k_{eff} is the effective thermal conductivity ($k+k_t$, k_t is the turbulent thermal conductivity), and J_j is the diffusion flux of the species j. $\boldsymbol{S_h}$ includes the heat of the chemical reaction and the source term. In the above equation

$$E = h - \frac{p}{\rho} + \frac{u_i^2}{2} \tag{5.5}$$

where sensible enthalpy h is defined for ideal gases as

$$h = \sum_{j'} m_{j'} h_{j'}$$

where $m_{j'}$ is the mass fraction of the species j' and

$$h_{j'} = \int_{T_{ref}}^{T} C_{p,j'} dT \tag{5.7}$$

where T_{ref} is 298.15 K

7. Turbulence Modelling

Turbulence is modeled using RNG k-ε model. The RNG based k-ε turbulence model provides both accuracy and efficiency in the modeling of turbulent flows. This model follows the two equation turbulence modeling framework and has been derived from the original governing equations for fluid flow using mathematical techniques called Renormalization Group (RNG) due to Yakhot and Orszag (1986). The RNG model provides a more general and fundamental model and is expected to yield improved predictions of near wall flows, separated flows, flows in curved geometries and flows that are strained by effects such as impingement or stagnation. In RNG k-ε model, more terms appear in the dissipation rate in transport equation, including a rate of strain term, which is important for treatment of flows in rapid distortion limit such as separated flows and stagnation flows. These features make the RNG k-ε model more accurate and reliable especially for swirling flows.

8. Reacting Flow Modeling (PDF Modeling Approach)

This is a non-premixed modeling approach and involves the solution of transport equations for one or two conserved scalars (the mixture fractions). Equations for the individual species are not solved. Instead, species concentrations are derived from the predicted mixture fraction fields. The thermo-chemistry calculations are preprocessed in prePDF and tabulated for look-up in FLUENT. Interaction of turbulence and chemistry is accounted for with a probability density function (PDF). The main advantage of this model is that it allows intermediate species prediction, dissociation effects and rigorous turbulence-chemistry coupling.

9. Results and Discussion

9.1 Non-reacting flow analysis :

Even though it is a time consuming process to model all the holes, it is the best method for capturing realistic flow field. Computer resources used is Intel Pentium IV processor with 1GB RAM memory, Windows 2000 Operating system. Even with real hole modeling it took only about 120 hours for reaching the convergence, with the above configuration of the computer.

Figure10 shows the location of plane at 0^0, 10^0 and 20^0. Figure 11 shows the magnitude of velocity vector (prediffuser inlet velocity of 178.65 m/s) from the compressor exit to turbine inlet for non-reacting flow condition at midplane (10^0 plane). Figure 11 shows clearly the recirculation, primary and dilution penetrations.

Two recirculation zones are formed at the corners in the dump diffuser region (Fig. 12) and this is due to the sudden expansion of the flow near that region. Airflow from compressor first enters the prediffuser with a high velocity. In the prediffuser the flow is decelerated and the reduction in velocity

head, which is converted to a rise in static pressure. Flow from prediffuser gets split into three branches: two streams that feed the outer and inner combustor annuli. Airflow in the outer and inner annuli then enters the flame tube through the primary and dilution holes. It can be seen that the recirculation is generated downstream of the combustor due to toroidal flow reversal created by the swirler and due to the interaction of opposing primary jets. Zoomed view of toroidal flow reversal is shown in Fig. 12 and it depicts the possibility of entrainment and recirculation of a portion of hot combustion products to mix with incoming air and fuel. This in turn helps to slow down the flow entering the core region and thus to stabilize the flame. Velocity vectors at axial plane through primary and dilution holes are shown in Fig. 13 and Fig. 14. The product of combustion, which is at higher temperature, is diluted through the air that is coming through dilution holes and results in a temperature that is acceptable to turbine blades.

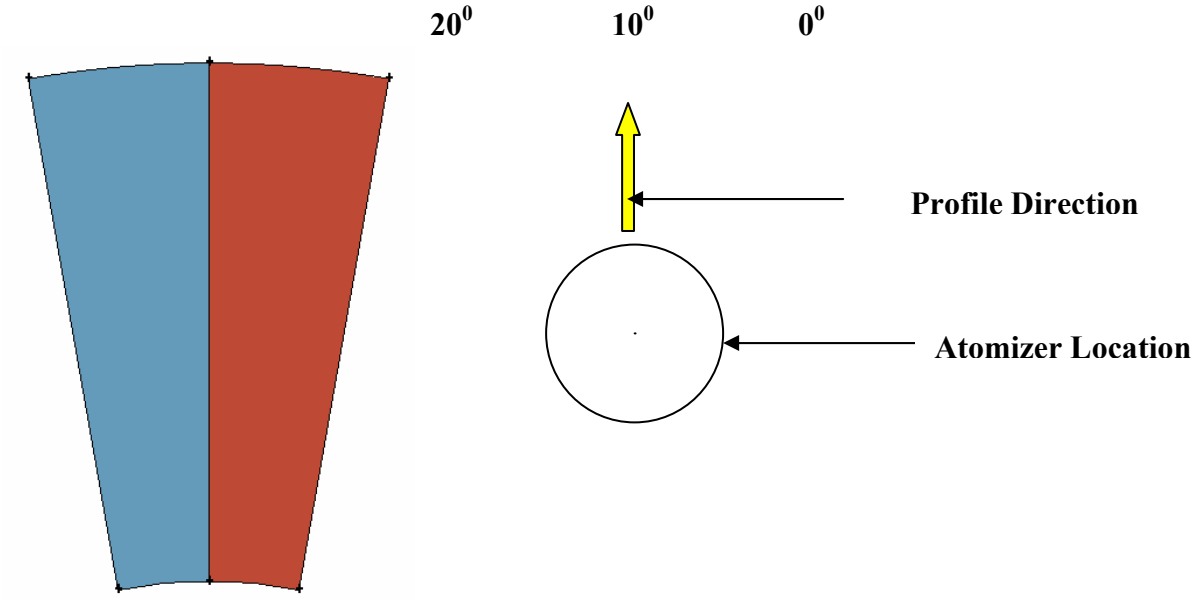

Figure 10: 20-Degree Sector Indicating the Cross-Sectional Plane Location

Total pressure contour is shown in Fig. 15. The total pressure drop across the combustor is due to various blockages like the atomizer mount and swirler. The pressure drop is due to the flow across the primary and dilution holes, cooling holes, dome and flare holes and also due to the skin friction drag along the walls of combustor casing. As the flow passes through the holes, the flow velocity increases resulting in total pressure drop due to the constricted passage. Table 1 shows the total pressure loss at various locations. It has been found that an increase in velocity of about 37% (158.8 to 218.35 m/s) results in increase in total pressure loss of about 86%.

9.2 Reacting flow analysis

Combustion analysis has been carried out for the geometry under consideration using heptane as fuel. Initially the reacting flow analysis has been carried out with following input:

SMD = 30 μ , Fuel injection velocity = 100 m/s, temperature = 373 ^{0}K
SMD = 70 μ , Fuel injection velocity = 100 m/s, temperature = 373 ^{0}K
SMD = 70 μ , Fuel injection velocity = 80 m/s, temperature = 373 ^{0}K

In all the above cases it has been found that the combustion is not occurring in the primary zone and is occurring in the dilution zone and in the exit of the combustion chamber. This is mainly due to the droplets that are escaping from the primary zone and getting trapped in the dilution zone and in the exit. In other words we can say that the fuel is not vaporized in the primary zone. The reason is that the latent heat of vaporization of heptane is 32 kJ/kg which is very high. For combusting, the fuel requires high surrounding temperature to reach its ignition point.

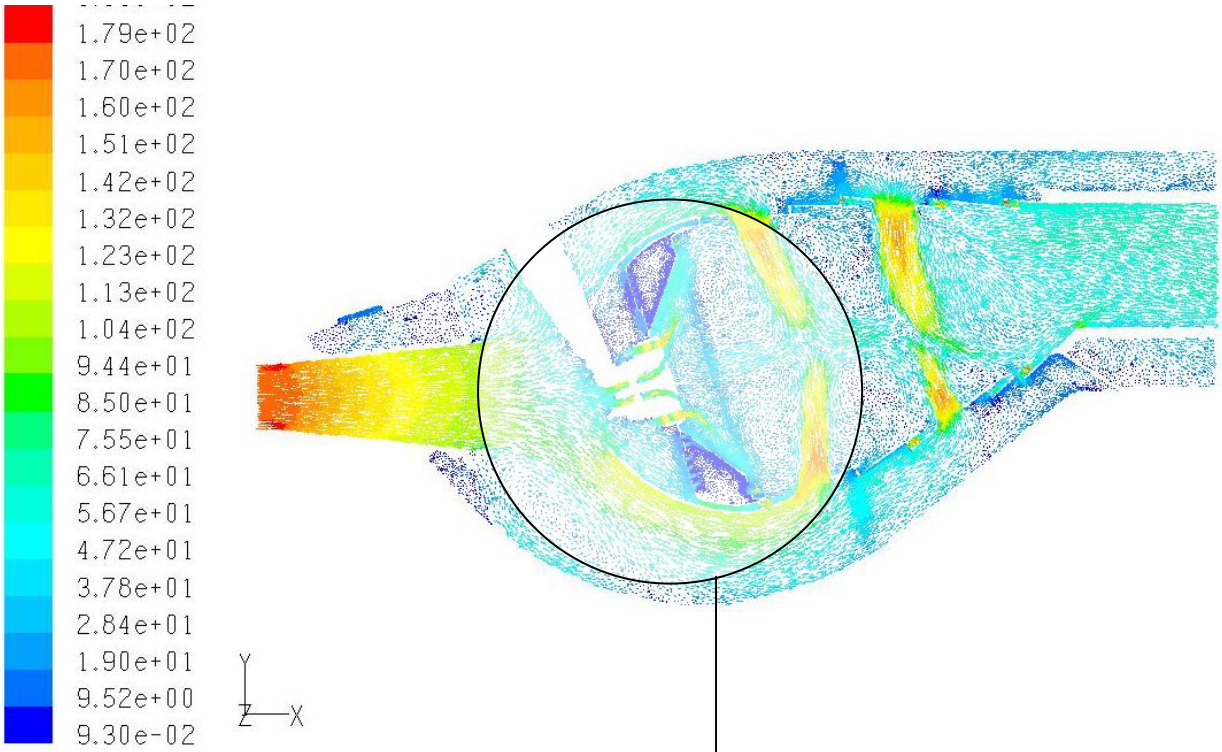

Figure 11: Velocity vector shown for mid-plane (10^0) for non-reacting case

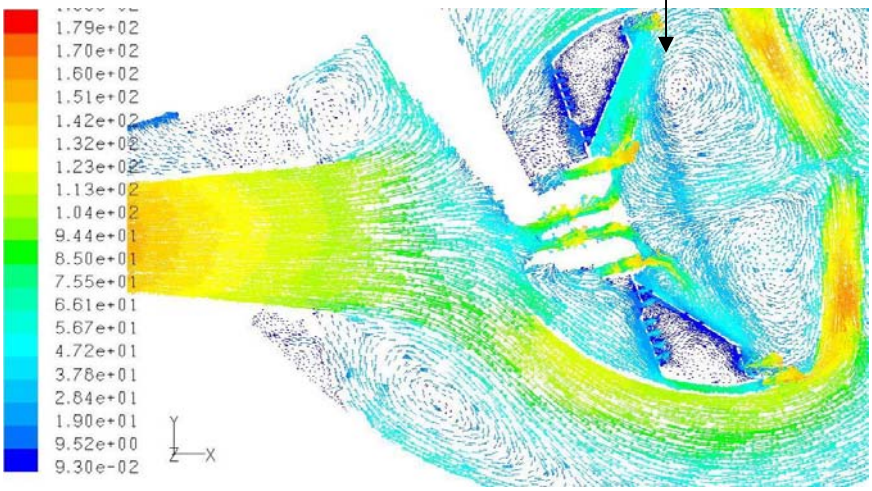

Figure 12: Zoomed view of velocity vector near diffuser downstream and primary zone

Total pressure contour for reacting flow case is shown in Fig. 16. The total pressure loss across the combustor increases from 6.3% for isothermal flow case to 6.55% for the reacting flow. This can be attributed to the additional drag losses incurred in view of the sudden acceleration of fluid due to combustion in the primary zone. The total temperature contour is shown in Fig. 17. It is seen that the preheating of fuel resulting in increasing in the temperature of primary zone. Because of the toroidal flow in the primary zone, complete mixing of fuel and air takes place which results in proper combustion. It produces mass weighted average temperature of 2760^0 K in the primary zone which is lesser than adiabatic flame temperature of the heptane-air mixture, when preheated. Thereafter it gradually reduces in the secondary zone and at the exit. The temperature in the secondary zone and at

the exit is higher but they are lower than that of primary zone. The reason may be due to the high preheat temperature of the fuel. Mass fraction contours of CO and CO_2 are shown in Fig. 18 and Fig. 19. Mass fraction of CO shows that there is absolutely no CO at the exit of the combustor. Complete combustion results in formation of CO_2. We can see the concentration of CO_2 in the primary zone, dilution zone and at the exit to ensure complete combustion.

In order to have combustion in the primary zone as per the requirement, fuel should vaporize in the primary zone. This is possible by preheating the fuel to higher temperature (746^0 K). Combustion was also carried out using Jet-aviation fuel which results in proper combustion inside combustion chamber. Keeping 746^0 K as inlet fuel temperature, inlet temperature of air = 895^0 K, mass flow rate of fuel = 1.9434 kg/s, Sauter mean diameter = 70 μ, fuel injection velocity = 80 m/s, combustion analysis was carried out.

It is found that the average exit velocity of the combustor increases from 60 m/s for isothermal case to 124 m/s for reacting flow case. This increase in velocity is due to the combustion of fuel air mixture in the flame tube and also due to the volume expansion of the liquid.

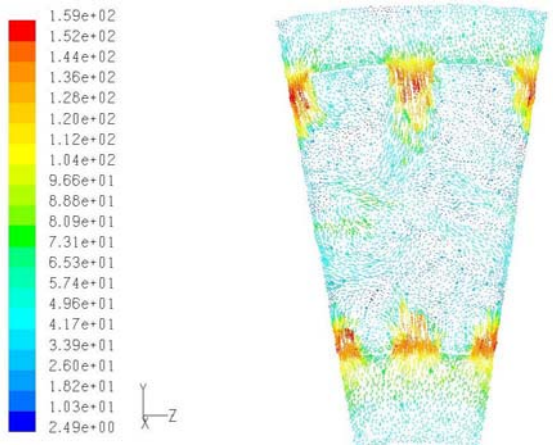

Figure 13: Flow through primary holes plane for non-reacting case

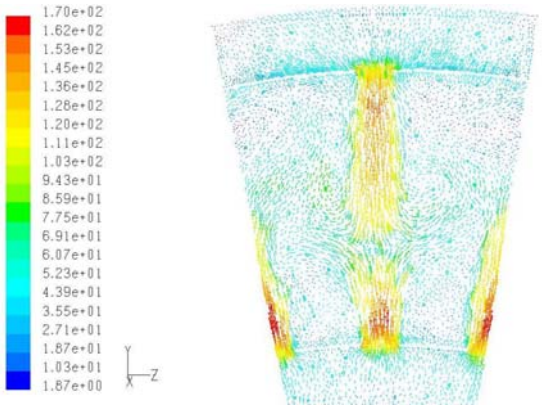

Figure 14: Flow through dilution holes plane for non-reacting case

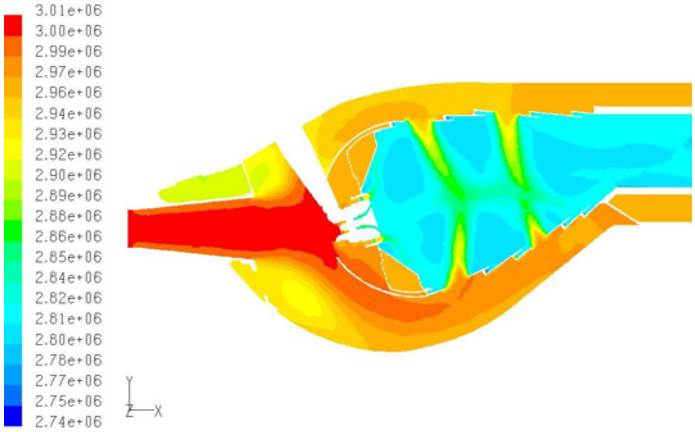

Figure 15: Total pressure contour for non-reacting case

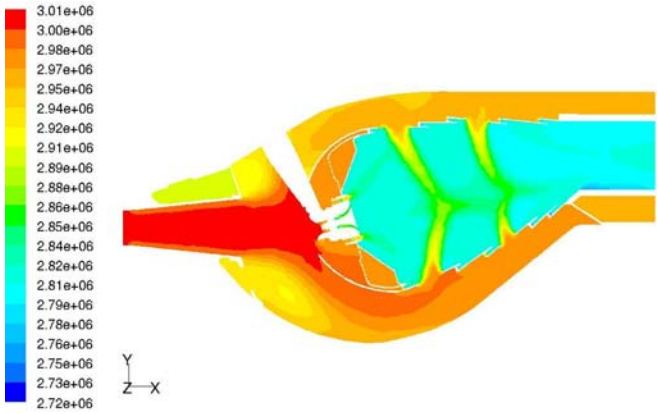

Figure 16: Total pressure contour for reacting flow

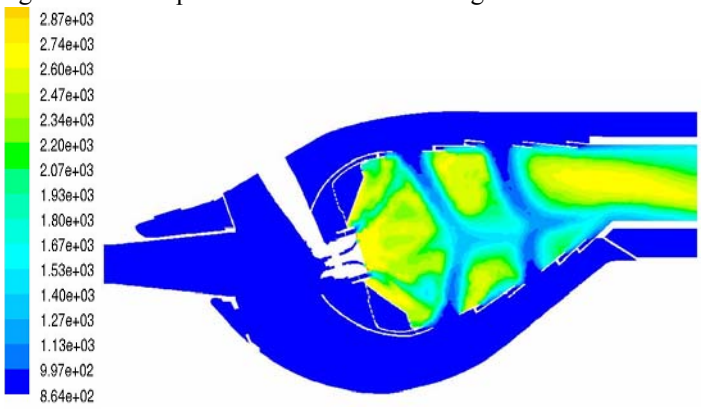

Figure 17: Total temperature contour for reacting flow

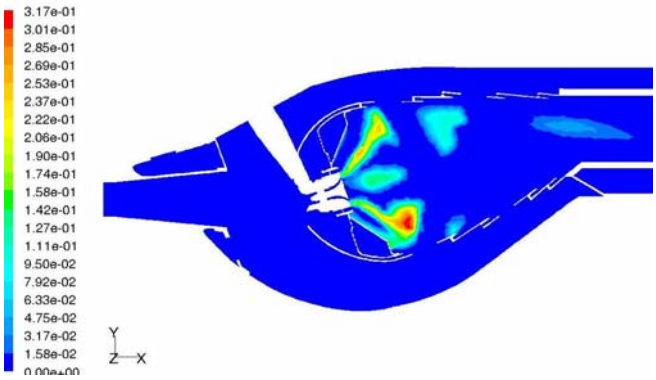

Figure 18: Mass fraction contour of CO

Table 1: Total pressure loss at three different locations

Location	% Pressure loss
Outlet	6.4
Plane along primary holes	3.23
Plane along dilution holes	4

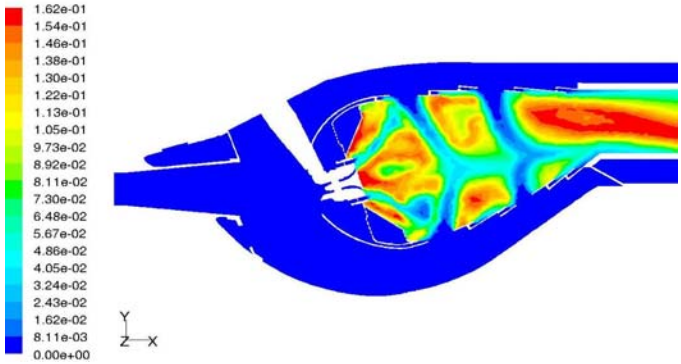

Figure 19: Mass fraction contour of CO_2

10. Conclusion

Numerical prediction has been carried out for non-reacting and reacting flow in a typical marine gas turbine combustor for three-dimensional configuration. Holes in the dome region, flare region, primary and dilution holes and in the liners are modeled. Non-reacting and reacting flow studies are carried out. Re-circulation zone is formed due to the effect of the radial pressure gradient created by the swirler and due to the interaction of opposing primary and dilution jets. Increase of 37% in the inlet velocity increases the total pressure loss of about 86%. The reacting flow analysis reveal that the overall pressure loss across the combustor and the exit velocity increases over that for the isothermal condition for the same inlet conditions, which is attributed to the additional turbulence generated and due to rapid addition of the energy due to combustion of fuel being injected.

References

Alizadeh, S., A. Askari, R. Benodekar, A. Ghobadian, and R. Sanatian (1996) CFD simulation of combustion in a model gas turbine combustor, *Third International Conference on Computers in Reciprocating Engines and Gas Turbines*, C499/060/96, 79-87.

Agarwal, A.K., J.S. Kapat, and T.T. Yang (1998) An Experimental/ computational study of airflow in the combustor-diffuser system of a gas turbine for power generation, *Transactions of the ASME*, 120, 24-33.

Balasubramaniam, V., and V.Ganesan (2001) Modelling of Combustion in a Gas Turbine Combustion System, 2nd International SAE India Mobility Conference, IIT-MADRAS, Chennai, Jan, 187-194.

Cameron, C.D., J. Brouwer, C.P. Wood, and G.S. Samuelsen (1989) A detailed characterization of the velocity and thermal fields in a model can combustor with wall jet injection, *Journal of Engineering for Gas Turbines and Power*, 111, 31-34.

Costura, D.M., P.B. Lawless, and S.H. Fankel (1999) A computational model for the study of gas turbine combustor dynamics, *Journal of Engineering for Gas Turbine and Power*, **121**, 243-248.

Ganesan, V., and D.B. Spalding (1979) Numerical Modelling of Combustion of Fuel Sprays in 3D Can Combustors, *Proc. 4th Symp.(Int) on Air Breathing Engines*, USA, 177-186.

Han, Y.M, W.S. Seol and D.S Lee (2001) Effects of fuel nozzle displacement on pre-filming airblast atomization, *Journal of Engineering for Gas Turbine and Power*, 123, 33-40.

Issac, K.M., and C. K. Wu (1989) Effect of swirl on axisymmetric sudden expansion flow, AIAA/ASME/SAE, *25th Propulsion Conference, Monterey*, July 10-12, pp.1-11.

Karki, K.C., V.L. Oechsle, and H.C. Mongia **(**1992) A computational procedure for diffuser combustor flow interaction analysis - *Journal of engineering for gas turbine and power*, 114/1,1-7.

Marouan, A.A., Nazha, and Hobina Rajakaruna (2000) An effective property, LHF-Type model for spray combustion, *Journal of Engineering for Gas Turbines and Power***,** 122, 275-279.

Mongia, H.C., R.S. Reynolds, and R. Srinivas (1992) Multidimensional gas turbine combustion modeling application and limitations, *AIAA Journal*, 890-902.

Novick, A.S., G.A. Miles, and D.G. Lilly (1979) Numerical simulation of combustor flow and fields: A primitive variable design capability, *Journal of Energy*, Article No.78-949, 95-103.
Sampath, S., and V. Ganesan (1987) Numerical prediction of flow and combustion in three dimensional gas turbine combustor, *J. of Inst. Energy*, **60**, 13-28.
Sokolov, K.Y., A.G. Tumanovsky, M.N. Gutnik, A.V. Sudarev, Y.I. Zakharov, and E.D. Winogradov (1995) Mathematical modeling of an annular Gas turbine combustor, *Journal of Engineering for gas turbine and power*, **117**, 94 - 99.
Tolpadi, A.K., I.Z. Hu, S.M. Correa, and D.L Burrus (1997) Coupled lagrangian monte carlo PDF-CFD computation of gas turbine combustor flow fields with finite-rate chemistry, *Journal of engineering for gas turbines and power*, 119, 519-526.